sustainability

MDPI

Article

Horizontal UHS Predictions for Varying Deep Geology Conditions—A Case Study of the City of Banja Luka

Borko Bulajić [1], Silva Lozančić [2], Senka Bajić [1,*], Dorin Radu [3], Ercan Işık [4], Milanka Negovanović [5] and Marijana Hadzima-Nyarko [2]

1 Faculty of Technical Sciences, University of Novi Sad, Trg Dositeja Obradovića 6, 21000 Novi Sad, Serbia; borkobulajic@uns.ac.rs
2 Faculty of Civil Engineering and Architecture Osijek, Josip Juraj Strossmayer University of Osijek, Vladimir Prelog St. 3, 31000 Osijek, Croatia; lozancic@gfos.hr (S.L.); mhadzima@gfos.hr (M.H.-N.)
3 Faculty of Civil Engineering, Transilvania University of Brașov, 500152 Brașov, Romania; dorin.radu@unitbv.ro
4 Department of Civil Engineering, Bitlis Eren University, Bitlis 13100, Türkiye; eisik@beu.edu.tr
5 Faculty of Mining and Geology, University of Belgrade, Đušina 7, 11120 Belgrade, Serbia; milanka.negovanovic@rgf.bg.ac.rs
* Correspondence: senka.bajic@uns.ac.rs

Abstract

In this study, we show how uniform hazard spectra (UHS) can contribute to sustainable development in regions with frequent moderate to strong seismic events and a variety of deeper geological conditions, by reducing seismic risks and enhancing resilience. The case study region surrounds a site at Banja Luka, Bosnia and Herzegovina. Frequency-dependent scaling equations are presented. UHS spectra for Banja Luka are calculated utilizing regional seismicity estimations, deep geology data, and the regional empirical formulae for scaling different *PSA* amplitudes. The UHS amplitudes are compared with Eurocode 8 spectra. The results demonstrate that the ratios of the highest UHS amplitudes to the corresponding PGA values differ significantly from 2.5, which is the factor specified by Eurocode 8 for the horizontal ground motion. The results also suggest that the influence of deep geology on UHS amplitudes can outweigh local soil effects. For example, at the vibration period of 0.1 s, the largest site effects are obtained for deep geology when comparing the UHS amplitude at geological rock to that at intermediate sites. In this case, the deep geology amplification of 1.47 is 19% higher than the local soil amplification of 1.24 for the same vibration period at the stiff soil sites compared to the rock soil sites. The UHS obtained may be interpreted as preliminary for Banja Luka and other places with similar deep geology, local soil conditions, and seismicity. When the quantity of strong-motion data in the region increases significantly beyond what it is now, it will be possible to correctly calibrate the existing attenuation equations and obtain more reliable UHS estimates.

Keywords: uniform hazard spectra; regional attenuation equations; deep geological site surroundings; local soil conditions; Eurocode 8

Academic Editor: Claudia Casapulla

Received: 6 May 2025
Revised: 27 May 2025
Accepted: 23 June 2025
Published: 30 June 2025

Citation: Bulajić, B.; Lozančić, S.; Bajić, S.; Radu, D.; Işık, E.; Negovanović, M.; Hadzima-Nyarko, M. Horizontal UHS Predictions for Varying Deep Geology Conditions—A Case Study of the City of Banja Luka. *Sustainability* **2025**, *17*, 6012. https://doi.org/10.3390/su17136012

1. Introduction

The expression "deep geology" describes the geological conditions that exist beneath the local soil at depths greater than 100–200 m and up to several kilometers, depending on local stratigraphy [1]. As per Trifunac and Brady's classification [1], deeper geological conditions are defined as (geological) rocks, (deep) geological sediments, and complex (intermediate). Numerous researchers have used analytical and numerical methods to explore

the ground motion amplification caused by deep sedimentary basins [2–11]. Furthermore, a recent study indicates that high-frequency ground motion will be greater than expected in places containing outcrops of extremely hard and compact geological rocks such as granites or basalts [12]. However, traditional seismic hazard maps only take into account shallow geological conditions. This is because most empirical GMPEs only consider the effects of local soil for the top 30 m of the stratigraphic profile and ignore the impact of underlying geological conditions [13]. This is still a standard practice, despite research indicating that site resonance is not significantly influenced by the shear-wave velocity in the top 30 m of the local soil [14]. Furthermore, a series of recent microzonation investigations in the region of former Yugoslavia [15–18] found that deep geological conditions have a considerable impact on both long- and short-period waves.

The 2004 edition of Eurocode 8 [19] acknowledges the possible importance of geological conditions below the local soil, noting in Clause 3.1.2(1) that the National Annex can establish a classification scheme to account for deep geology conditions. However, just like all EU countries, Bosnia and Herzegovina has not incorporated deep geology into its ground classification scheme [20–22].

Table 1 displays the ground types according to Eurocode 8 [16]. The hazard map is represented by the horizontal PGA values for ground type A, a_g. As shown in Table 1, the highest spectral amplitudes are the products of a_g, a constant value of 2.5, and the soil factor that is greater than one for all ground types. Another objective of this study is to determine whether the 2.5 spectral acceleration factor (the ratio between the largest spectral amplitudes and corresponding PGA values), as specified by Eurocode 8, provides realistic estimations for the highest spectral amplitudes.

Table 1. Maximum horizontal *PSA* amplitudes and related vibration periods, *T*, defined for different ground types according to Eurocode 8 [19], with a_g being the horizontal PGA value taken from the associated seismic hazard map.

Eurocode 8 [19] Ground Types	**Type 1 EC8 Spectra: M_S > 5.5**	**Type 2 EC8 Spectra: $M_S \leq$ 5.5**
Ground Type A, $V_{S,30}$ > 800 m/s "Rock, at the surface up to 5 m of weaker material."	$a_g \times 2.5$ 0.15 s $\leq T \leq$ 0.40 s	$a_g \times 2.5$ 0.05 s $\leq T \leq$ 0.25 s
Ground Type B, $V_{S,30}$ = 360–800 m/s "At least several tens of meters thick deposits. Very dense sand, gravel, or very stiff clay."	$a_g \times 3.0$ 0.15 s $\leq T \leq$ 0.50 s	$a_g \times 3.375$ 0.05 s $\leq T \leq$ 0.25 s
Ground Type C, $V_{S,30}$ = 180–360 m/s "Deep deposits, several tens of meters up to hundreds of meters thick. Dense or medium dense sand, gravel, or stiff clay."	$a_g \times 2.875$ 0.20 s $\leq T \leq$ 0.60 s	$a_g \times 3.75$ 0.10 s $\leq T \leq$ 0.25 s
Ground Type D, $V_{S,30}$ < 180 m/s "Deposits. Loose-to-medium cohesionless soil, or predominantly soft-to-firm cohesive soil."	$a_g \times 3.375$ 0.20 s $\leq T \leq$ 0.80 s	$a_g \times 4.5$ 0.10 s $\leq T \leq$ 0.30 s
Ground Type E "Alluvium layer at the surface, between 5 and 20 m thick, above stiffer material. $V_{S,30}$ < 360 m/s."	$a_g \times 3.5$ 0.15 s $\leq T \leq$ 0.50 s	$a_g \times 4.0$ 0.05 s $\leq T \leq$ 0.25 s

Banja Luka is used as the case study area for varying deep geology and a history of devastating earthquakes. The fundamental purpose of this research is to evaluate the amplification (or perhaps de-amplification) impacts of deep geology on various spectral amplitudes and include these effects in PSHA estimates.

This paper begins by describing the regional seismicity and geological settings for the area surrounding the city of Banja Luka. It then proceeds to present regional GMPEs for horizontal *PSA* and compare them to actual records of strong motion in Banja Luka. Finally, UHS spectra at a site in Banja Luka are generated and compared to the corresponding Eurocode 8 spectra.

2. Regional Seismicity and Geological Settings

As seen in Figure 1, Banja Luka is located in northwest Bosnia and Herzegovina, between the Dinaric Alps and the Pannonian Basin. A recent study suggests that earthquakes in the region surrounding Banja Luka may be caused by the contractional reactivation of normal faults of Late Paleogene to Middle Miocene [23]. This fault reactivation postdates the deposition of the youngest Pannonian Basin strata of Pontian age [23]. The strongest reported past earthquake near Banja Luka occurred on 27 October 1969. It had a magnitude of M_w = 6.1, an epicenter 10 km northwest of Banja Luka (see Figure 1), and a focal depth of 15 km. The intensity in the epicentral region was VIII-IX °MCS (Mercalli–Cancani–Sieberg Macrosecismic Scale), while Banja Luka had VIII °MCS. After examining fault plane solutions for the 1969 Banja Luka earthquake, Ustaszewski et al. [23] suggested reverse faulting along ESE–WNW-striking nodal planes. Additionally, based on similar results for several minor earthquakes in the region, Ustaszewski et al. [23] found evidence of a continuous shortening in the interior Dinarides. Anyone interested in knowing more about Banja Luka seismotectonics should read this thorough study together with the *Geological Guidebook through Bosnia and Herzegovina* [24]. Figure 1 shows the epicenters of all $M_w \geq 3$ regional earthquakes between 1900 and April 2025 [25], including two recent destructive earthquakes in neighboring Croatia and the largest historical earthquakes in Bosnia and Herzegovina and Montenegro. The solid blue circle represents the researched location in Banja Luka. As seen in Figure 1, seismic activity in the Banja Luka area is higher than in the Pannonian Basin but smaller than along the Adriatic coast.

Banja Luka is located on the southwest border of the Pannonian Basin and the north border of the Dinaric Alps (see the top-left plot in Figure 1). The bottom-left plot in Figure 1 shows the spatial distribution of the deep geology parameters for an area surrounding the analyzed site (shown with a blue circle). This plot was modified from a previous microzonation study for Banja Luka [15] and was based on the geological map created by Mojičević et al. for Banja Luka and neighboring areas [26]. In this map, site geology was defined based on major lithostratigraphic formations and their depths, per the classification by Trifunac and Brady [1]—see Table 2. The site with coordinates 17°15′ E, 44°46.5′ N, was chosen as a case study because it is surrounded by different deep geology types. To the west of the analyzed site, a lower terrace of Vrbas River lies atop marls, clays, and sands; to the north, we can find a metamorphic ophiolitic melange formation; to the east, an outcrop of a spilite formation can be found. For a detailed description of the Banja Luka geological features, please see [14,24,27,28].

The map detailing the deep geological parameters for the examined area sets the basis for seismic microzonation. However, we must first select suitable ground motion prediction equations. The GMPEs used in this study are presented in the next section.

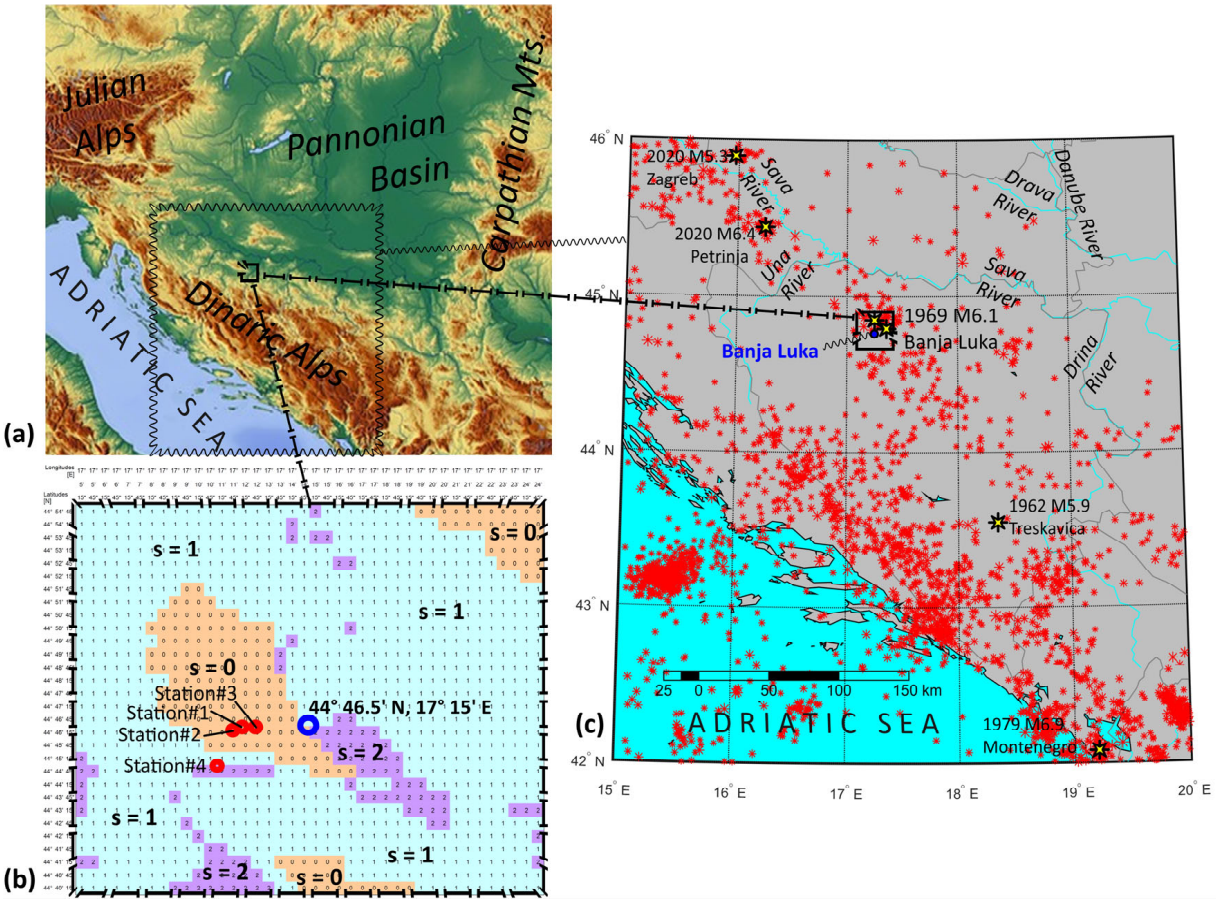

Figure 1. (**a**)—Pannonian Basin and Dinaric Alps, (**b**)—epicenters of regional earthquakes with $M_w \geq 3.0$ [25], with a few of the largest historical earthquakes in the region and two recent devastating earthquakes in Croatia, (**c**)—distribution of the parameters that define deep geology types according to [1] ($s = 0$ for sediments, $s = 1$ for complex geological conditions, and $s = 2$ for geological rock) for the area between 17°05′ E and 17°25′ E, and between 44°40′ N and 44°55′ N, modified from [15]. Blue circle designates the investigated location. Four accelerograph stations in Banja Luka, which recorded strong motion accelerograms in the past, are indicated by red circles.

Table 2. Categorical variables used in Equation (1) for deep geology (S_{G1}/S_{G2}) and local soil (S_{L1}/S_{L2}).

Shallow Geology Categorical Variables	Shallow Geology Type	Deep Geology Categorical Variables	Deep Geology Type
$S_{L1} = S_{L2} = 0$	"Rock" soil: $s_L = 0$	$S_{G1} = S_{G2} = 0$	Basement (geological) rock: $s = 2$
$S_{L1} = 1$ and $S_{L2} = 0$	Stiff soil: $s_L = 1$	$S_{G1} = 1$ and $S_{G2} = 0$	Intermediate sites: $s = 1$
$S_{L1} = 0$ and $S_{L2} = 1$	Deep soil: $s_L = 2$	$S_{G1} = 0$ and $S_{G2} = 1$	Deep geological sediments: $s = 0$

3. GMPEs for *PSA* in Areas with Varying Deep Geology

In this section, we present regional GMPEs for the prediction of *PSA* in areas with diverse deep geological conditions. We will use the following mathematical expression:

$$log[PSA(T)] = c_1(T) + c_2(T) \cdot M + c_3(T) \cdot log\left(\sqrt{R^2 + R_0(T)^2}\right) + c_4(T) \cdot S_{L1} + c_5(T) \cdot S_{L2} + c_6(T) \cdot S_{G1} + c_7(T) \cdot S_{G2} + \sigma_{log}(T) \cdot P. \quad (1)$$

Here, $PSA(T)$ represents horizontal PSA spectra (in [g]), T represents vibration period, M represents magnitude, and R represents epicentral distance (in [km]) (we also developed equations for hypocentral distance [8,9]). Categorical variables S_{L1}, S_{L2}, S_{G1}, and S_{G2} are described in Table 2. Shallow geology is separated into three local soil types: rock, stiff soil, and deep soil, in compliance with Seed et al.'s classification [27,28], taking into consideration depths more than 30 m. In Table 2, the term "rock" soil is used to characterize soils with a soil layer thickness of less than 10 m, above the layer with $V_S > 800$ m/s. Stiff soil defines sites with a 15–75 m deep soil layer on top of a $V_S > 800$ m/s layer. Finally, deep soil characterizes more than 100 m thick layers of soil above the $V_S > 800$ m/s layer. We assumed a log-normal distribution of the data, and σ_{log} represents the standard deviation, calculated for the common logarithm of PSA, and ε is 0 for the median estimates and ± 1 for the median $\pm\sigma_{log}$ estimates.

It should be mentioned that the region of former Yugoslavia is one of few regions worldwide where data on deep geology were compiled for many recording stations. It has been shown that spectral predictions based on GMPEs that concurrently take into account every site category indicated in Table 2 exhibit excellent agreement with actual ground motion recordings and reported intensities [9,12,15,29].

The database of strong-motion records that were used to derive the GMPEs comprises 436 horizontal components of acceleration time histories recorded solely in the region of former SFRY from 112 earthquakes with magnitudes between 3 and 6.8 [30–32]. Detailed information on this data can be found in [8,9,33] and will not be repeated here.

Scaling coefficients were computed by multiple linear regression analyses. For each vibration period, R_0 from Equation (1) was iteratively changed to maximize the R^2 statistics. The MATLAB® scripts for computing the scaling coefficients shown in Tables A1 and A2 were prepared in MATLAB® (release 2015a of version 8.5), using the function "regress" to perform multiple linear regression analyses and the function "smooth" to smooth the scaling coefficients by weighted linear least squares using a second-degree polynomial model. In Appendix A, we present scaling coefficients for 61 vibration periods in Table A1. Because more than half of the data were recorded at shorter distances, we performed another set of analyses using only data at source-to-site distances up to 30 km. The resulting scaling coefficients are also given in Appendix A, in Table A2.

PSA attenuation with distance for six vibration periods (0.05, 0.10, 0.30, 0.50, 1.00, and 2.00 s) is shown in Figures 2 and 3. Figure 2 shows empirical PSA predictions for different types of deep geology and rock as the local soil ($s_L = 0$). Figure 3 shows how PSA changes with types of local soil when type of deep geology (s) remains the same. In both figures, solid lines show the PSA estimations based on all data (scaling coefficients from Table A1), and dashed lines depict the empirical spectral estimates based only on the data recorded at shorter distances (see Table A2).

The c_4, c_5, c_6, and c_7 scaling coefficients from Equation (1) can be used to find ratios between the $PSA(T)$ for different site conditions. More precisely, we can calculate ratios between the PSA estimates at stiff soil ($s_L = 1$) and rock soil ($s_L = 0$) by calculating 10^{c4}. Vice versa, the ratio between PSA estimates at rock soil ($s_L = 0$) and stiff soil ($s_L = 1$) is calculated as $1/10^{c4}$. The ratios between deep soil ($s_L = 2$) and rock soil ($s_L = 0$) PSA estimates are calculated as 10^{c5}. The same calculation also applies to the deep geology effects. The ratios between intermediate deep geology sites ($s = 1$) and geological rock ($s = 2$) PSA values are calculated as 10^{c6}, while the ratios between deep geological sediments ($s = 0$) and geological rock ($s = 2$) can be calculated as 10^{c7}. Table 3 summarizes empirical ratios between the $PSA(T)$ for different local soil or deep geology conditions, which were calculated for eight different vibration periods using scaling coefficients from Table A1.

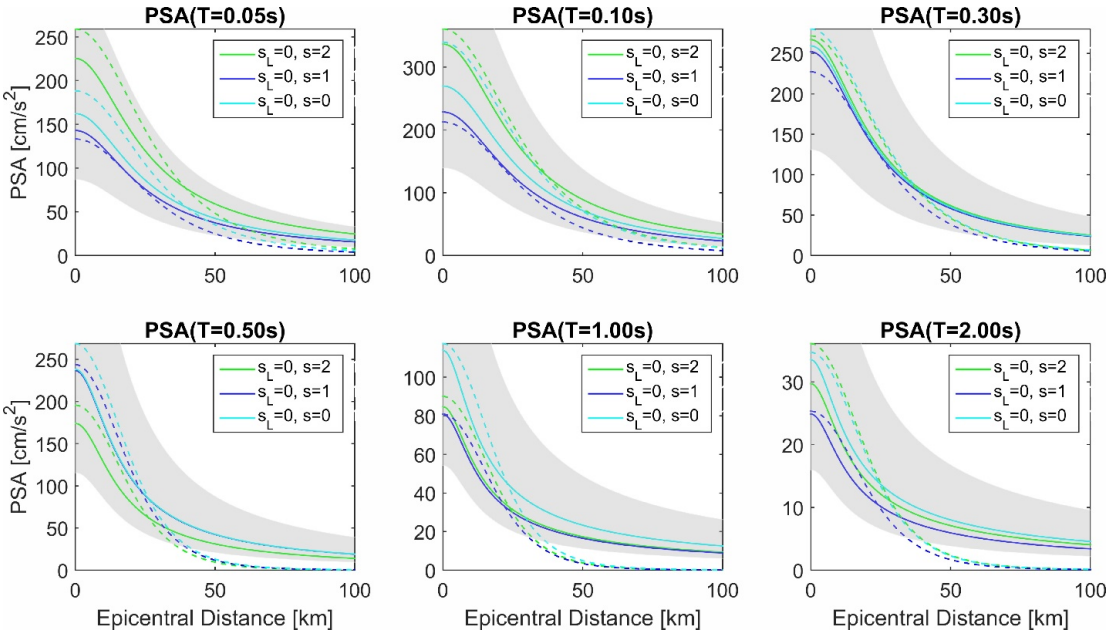

Figure 2. GMPEs for six vibration periods, T, computed by Equation (1) and the scaling coefficients from Table A1 (solid lines) and Table A2 (dashed lines), for rock as the local soil type (s_L = 0) and three different deep geology types (see Table 2). The gray area designates the median $\pm\sigma_{log}$ empirical estimates (68% confidence interval) for s = 0.

For example, if we use the scaling coefficients that are given in Table A1, *PSA* for T = 0.05 s (which can be viewed as an upper boundary for PGA values) are $1/10^{-0.143}$ = 1.39 times and $1/10^{-0.198}$ = 1.58 times larger for the deep geology rocks (s = 2) than for the sediments and intermediate geology (s = 1), respectively. A similar result is obtained for T = 0.10 s when the s = 2 *PSA* estimates are $1/10^{-0.096}$ = 1.25 and $1/10^{-0.168}$ = 1.47 times larger than the s = 0 and s = 1 ones. This is most likely due to the fact that short-period waves travel through more compact rocks (like granite and basalt) faster. In contrast, the *PSA* estimations for T = 1.0 s are $10^{0.129}$ = 1.35 times larger in geological sediments than in geological rock.

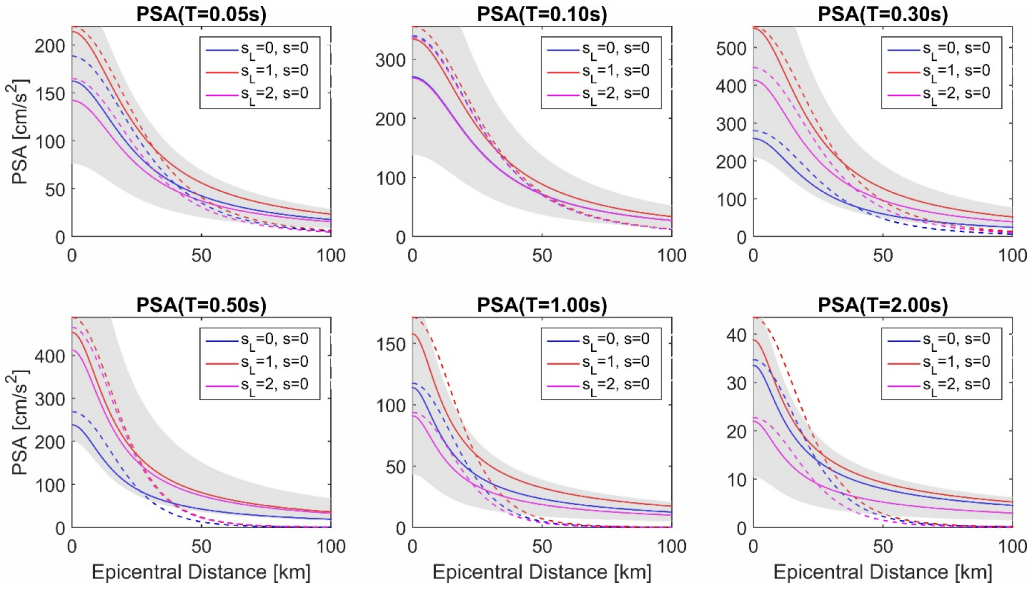

(**a**)

Figure 3. *Cont.*

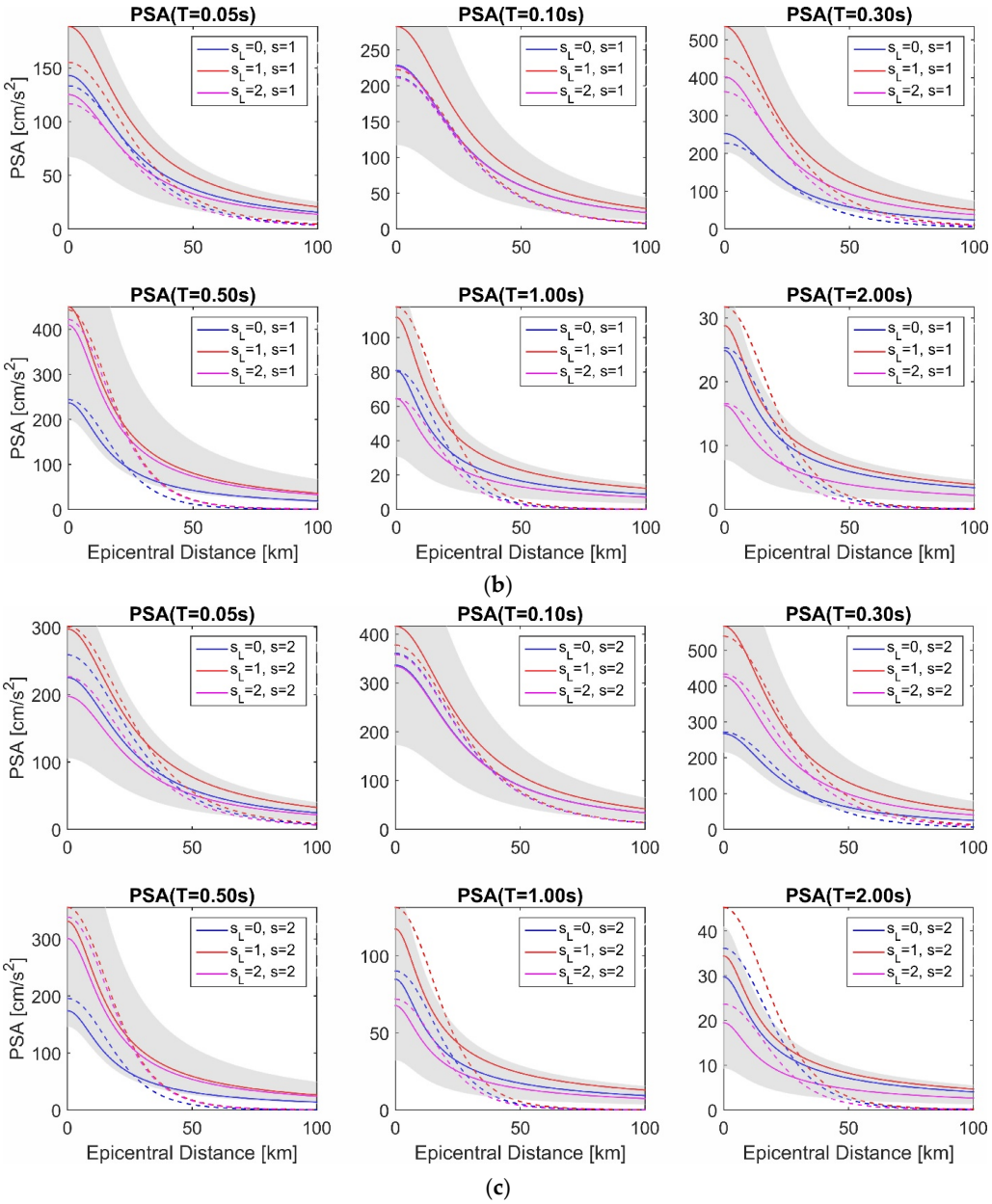

Figure 3. (**a**). GMPEs for six vibration periods, T, computed by Equation (1) and the scaling coefficients from Table A1 (solid lines) and Table A2 (dashed lines), for deep geological sediments (s = 0) and three different local soil parameters, s_L (see Table 2). The shaded area designates the median $\pm\sigma_{log}$ empirical estimates (68% confidence interval) for s_L = 2. (**b**). GMPEs for intermediate deep geology (s = 1) and three different local soil parameters, s_L. (**c**). GMPEs for geological rock (s = 2) and three different local soil parameters, s_L.

If we now focus on the local soil, we can see that *PSAs* at T = 0.05 s and T = 0.10 s will be lower for deep soil (s_L = 0) than for the rock sites (s_L = 0), because $10^{-0.058}$ equals 0.88 and $10^{-0.003}$ is 0.93. This indicates that, due to the nonlinear behavior of soft and deep sediments under strong ground motion, energy dissipation in deep soil outweighs the amplification of short-period waves. However, this is not the case for all vibration periods. For example, *PSA* for T = 0.40 s is $10^{0.248}$ = 1.77 times larger for deep soil sites than for the rock sites.

Table 3. Empirical ratios between the *PSA*(*T*), calculated using scaling coefficients from Table A1 for different local soil (c_4/c_5) and deep geology (c_6/c_7) conditions.

	Stiff Soil s_L = 1/ "Rock" Soil s_L = 0	**"Rock" Soil s_L = 0/ Stiff Soil s_L = 1**	**Deep Soil s_L = 2/ "Rock" Soil s_L = 0**	**"Rock" Soil s_L = 0/ Deep Soil s_L = 2**	**Intermed. Sites: s = 1/ Geological Rock: s = 2**	**Geological Rock: s = 2/ Intermed. Sites, s = 1**	**Deep Geol. Sediments: s = 0/ Geological Rock: s = 2**	**Geological Rock: s = 2/ Deep Geol. Sediments: s = 0**
T [s]	10^{c4}	$1/10^{c4}$	10^{c5}	$1/10^{c5}$	10^{c6}	$1/10^{c6}$	10^{c7}	$1/10^{c7}$
0.05	1.32	0.76	0.88	1.14	0.63	1.58	0.72	1.39
0.10	1.24	0.81	0.99	1.01	0.68	1.47	0.80	1.25
0.20	1.80	0.55	1.30	0.77	0.63	1.60	0.65	1.54
0.30	2.12	0.47	1.60	0.63	0.94	1.06	0.97	1.03
0.40	2.08	0.48	1.77	0.57	1.26	0.79	1.22	0.82
0.50	1.90	0.53	1.73	0.58	1.36	0.74	1.37	0.73
1.00	1.38	0.72	0.80	1.25	0.95	1.05	1.34	0.74
2.00	1.16	0.86	0.65	1.53	0.84	1.19	1.13	0.89

Table 3 shows that, depending on the vibration period, the effects of deep geology may outweigh the effects of local soil. For example, for T = 0.1 s, the largest site effects are obtained for deep geology when comparing the *PSA* at geological rock to that at intermediate sites. Compared to the local soil amplification for the same vibration period at the stiff soil sites, 1.24, the deep geology amplification is 1.47, 19% higher.

Furthermore, we can also calculate the coupled effects of local soil and deep geology. As shown in our previous study for Osijek, Croatia [9], which focused only on the deep soil atop deep geology sediments, *PSA*(*T*) for such a combination of site conditions can be compared to that at the rock (local) soil atop geological rock by calculating $10^{c5} \cdot 10^{c7}$. As shown in [9], for short-period spectra we obtain around 37% drop in deep soils atop deep geological sediments. If we use scaling coefficients from Table A1, for T = 0.05 s, we can find an exactly 37% drop in *PSA*, as $10^{-0.058} \cdot 10^{-0.143} = 0.63$. Vice versa, we can also calculate the combined amplification effects when analyzing *PSA*(T = 0.05 s) at stiff soil atop geological rock, and comparing it to that at rock soil and intermediate sites. In this case, we can calculate the corresponding ratio as $10^{c4} \cdot 1/10^{c6} = 10^{0.120} \cdot 1/10^{-0.198} = 2.08$.

Figure 4 presents a comparison between the empirical *PSA* predictions (derived from Equation (1) and the scaling coefficients from Tables A1 and A2) and the "real" spectra of both horizontal components of 18 accelerograms that were recorded by four accelerograph stations [30] in Banja Luka (see Figure 1). It can be seen that there is a high degree of agreement between the predicted and actual spectra.

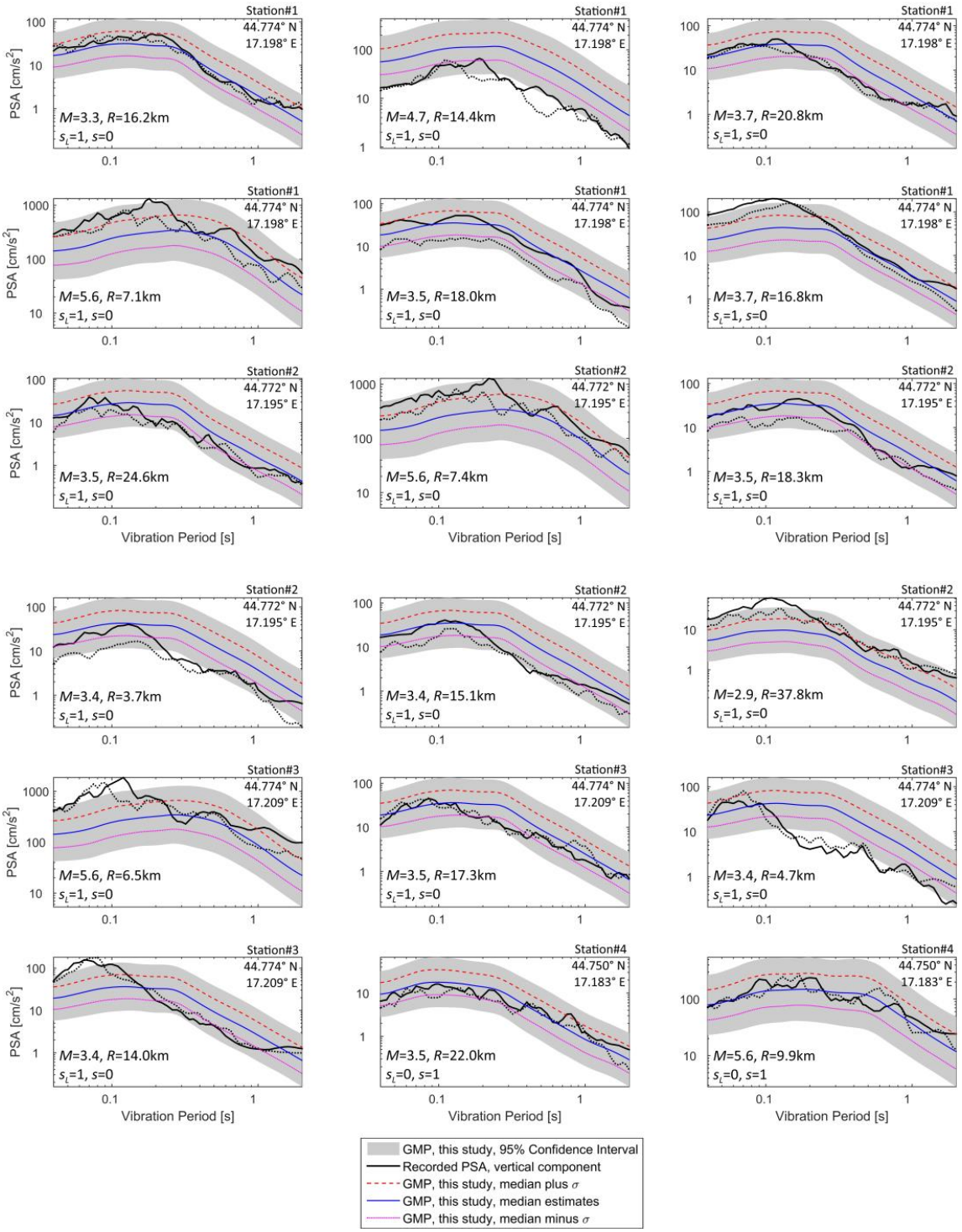

Figure 4. Comparison of the empirical *PSA* predictions derived from Equation (1) and the coefficients in Tables A1 and A2 with regional horizontal spectra recorded at four different sites in Banja Luka (refer to Figure 1).

4. Uniform Hazard Spectra for a Location in Banja Luka

In the following section, we carry out a PSHA analysis with Equation (1) as the GMPE and the scaling coefficients given in Table A1. We also use the SHARE (Seismic Hazard Harmonization in Europe) Project's pan-European seismic source zone model [34–36]. This model is based on "SHARE European Earthquake Catalogue" (abbreviated as SHEEC [37]), which is a homogenous earthquake catalogue established for the SHARE project. The

completeness, magnitude homogenization to M_w, and other significant factors of the SHEEC catalogue are described in detail in [35,38,39] and are not discussed here.

Figure 5 depicts the limits of the seismic source zones that were used in the hazard calculations for the 44°46.5′ N, 17°15′ E site in Banja Luka, as well as the epicenters of a few major historical and a few recent destructive seismic events in the northwestern Balkans [25]. Figure 5 also depicts the radii of 227, 160, 102, and 75.5 km, which are the distances that have to be included in the PSHA calculations to achieve 1% accuracy for 475-year return period UHS amplitudes at 1.0, 0.5, 0.3, and 0.1 s, respectively. Furthermore, the smallest circle, 38.25 km in radius, represents the distance that is needed for 10% accuracy in 475-year return period PSHA results for the 0.1 s UHS amplitude. The depicted distances (circles) demonstrate that short-period UHS amplitudes are dominated by local events and are less sensitive to the presence of distant severe earthquakes.

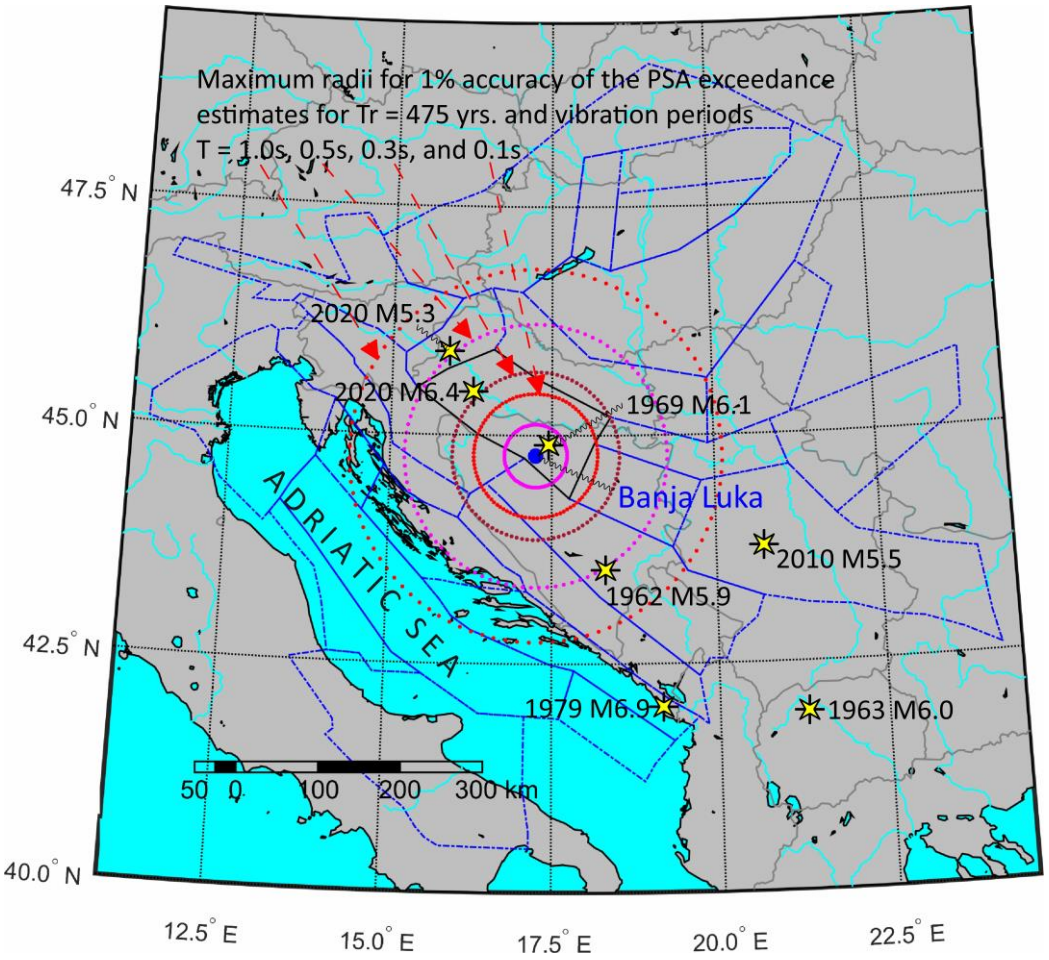

Figure 5. Areal source zones used to compute the seismic hazard. The largest four circles illustrate the maximum radii needed for capturing 1% accuracy of the UHS for the return period *Tr* = 475 years and vibration periods of 1.0, 0.5, 0.3, and 0.1 s. The circle with the smallest radius depicts the distance needed for capturing 10% accuracy of the UHS for the return period *Tr* = 475 years and a vibration period of 0.1 s.

The PSHA estimates were calculated using the REASSESS V2.1 software [40], which is based on Cornell [41] and McGuire's [42] methodologies. Mean yearly rate of occurrence, $N(a)$, of earthquakes that will lead a *PSA* amplitude to exceed expectation "*a*" is calculated as the sum of the products of probabilities that are associated with distance, magnitude recurrence, and the GMPE estimates, which were computed for all the given distances and

magnitudes. When a homogeneous Poisson distribution is considered, the probability that the expectation a will be surpassed at least once per year can be computed as follows [43]:

$$P(a) = 1 - e^{-N(a)}. \quad (2)$$

If we further take a binomial distribution into account, the probability that a *PSA* amplitude will surpass the expectation a at least once in t years can be approximated as follows [43]:

$$p(a) = 1 - [1 - P(a)]^t \quad (3)$$

What we usually call a return period, *Tr*, is a value that can be calculated as $N(a)^{-1}$ and does not correlate with any earthquake important from an engineering perspective. For example, *Tr* = 475 years is just the reciprocal value of $N(a)$ of approximately 0.002107 and corresponds to $p(a)$ = 10% in T = 50 years. This return period does not represent an earthquake that occurs every 475 years. The source-to-site distances and magnitudes of earthquakes contributing most to $N(a)$ can be calculated using "seismic hazard disaggregation" [44]. In the disaggregation, we may also specify the number of standard deviations that the calculated $\log(a)$ deviates from the mean empirical estimate for each magnitude and distance pair [45].

Figure 6 shows PSHA disaggregation at the 44°46.5′ N, 17°15′ E site, for different vibration periods and hazard probabilities of 10% in 10 and 50 years that correspond to 95-year and 475-year return periods, respectively. As expected, we can see that the contributing magnitudes increase with the vibration period and with the so-called return period. In Figure 7, the bottom-left plot and two top plots show cumulative PSHA disaggregation for distances and magnitudes. These plots also show that the prevailing distance increases with the vibration period. The bottom-right plot shows the recurrence curve for the areal source zone surrounding Banja Luka. This plot shows the "real" return periods for the vibration period of 0.1 s and three return periods (95, 475, and 2475 years) and for the vibration period of 1.0 s and a 475-year return period. These return periods were calculated for the magnitudes that contribute to 50% of the anticipated probabilities of exceedance. The actual return periods of these magnitudes (from top to bottom—4.75, 5.05, 5.4, and 5.7) are significantly shorter than the corresponding return periods, *Tr*. Though this might be a known property of hazard disaggregation for seismologists, for common civil engineers this is usually very confusing and may lead to erroneous decisions when choosing the spectral type based on the most contributing earthquakes. We should remember that Eurocode 8 [19] defines Type 1 and Type 2 spectra not based on maximum credible magnitudes but based on those magnitudes that "contribute most to the seismic hazard defined for the site for the purpose of probabilistic hazard assessment" (see Clause 3.2.2.1, (4), Note 2 and 3.2.2.2, (2)P, Note 1). In Bosnia and Herzegovina's National Annex to Eurocode 8 [20], the type of spectrum is not defined but left to users to choose, without providing them with the hazard disaggregation data. However, although in Banja Luka there is a history of earthquakes with magnitudes larger than 5.5, Figures 6 and 7 show that only for longer vibration periods, and longer *Tr*, the most contributing magnitudes are larger than 5.5. For PGA and shorter periods, these magnitudes are smaller than 5.5. Another problem is that the hazard maps that accompany Eurocode 8 are expressed only in terms of PGA. Hence, it is not clear how to properly define Type 1 or 2 in the Eurocode 8 [19] spectra. It is also not clear how to combine seismic hazard estimates with that of other hazards in the case of multi-risk analyses. For example, effects of a flood that occurs every 100 years cannot be combined with the earthquake effects that are estimated based on the 95-year map from the National Annex to Eurocode 8 [20], but rather with the seismic effects based on the hazard values given on the 475-year map [20].

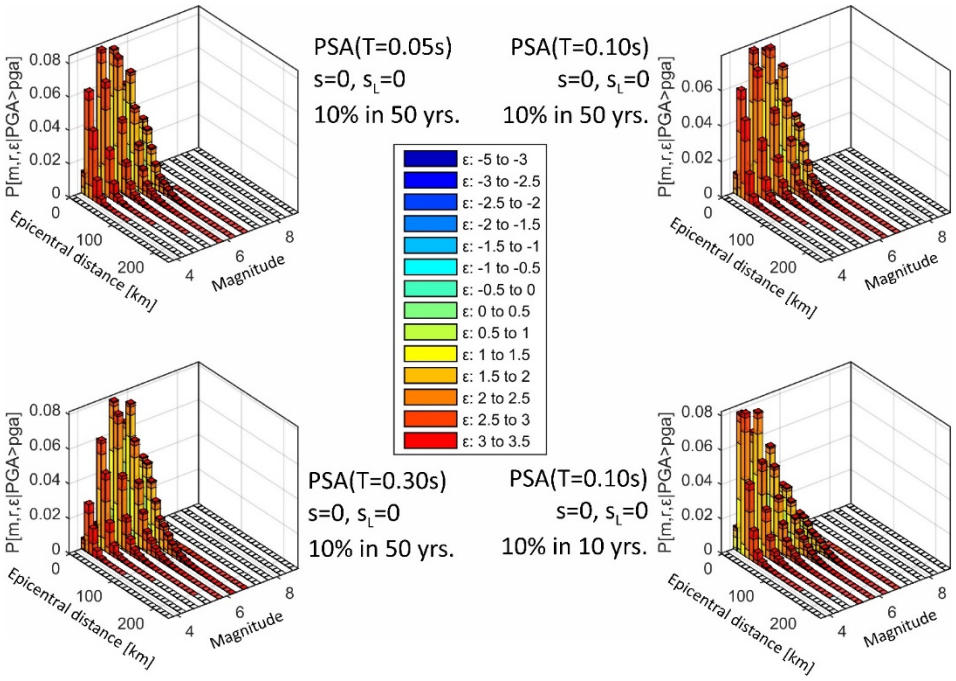

Figure 6. Disaggregation of seismic hazard for different vibration periods and hazard probabilities at the 44°46.5′ N, 17°15′ E site (see the solid blue circle in Figures 1 and 5).

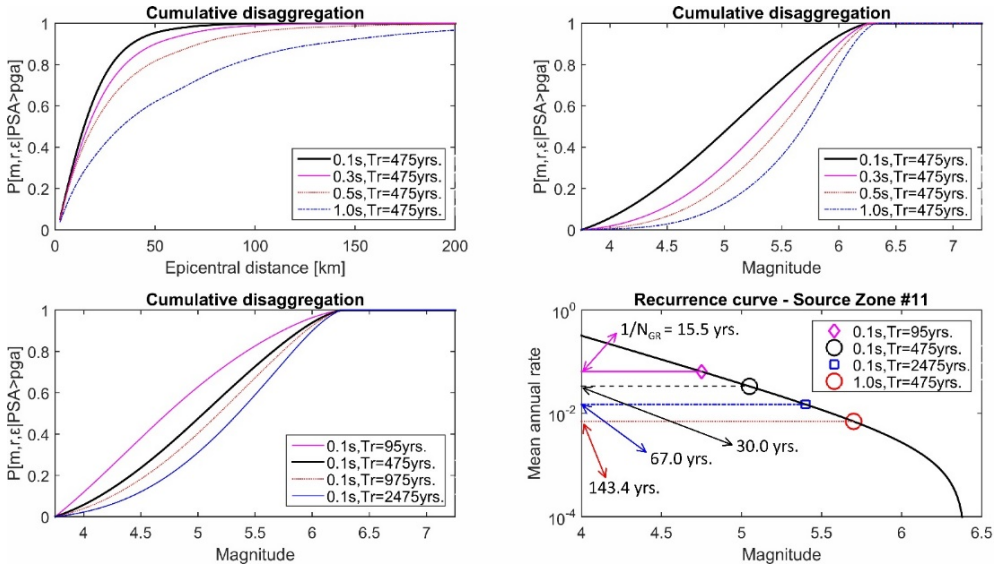

Figure 7. Cumulative disaggregation at the 44°46.5′ N, 17°15′ E site, calculated for distances and magnitudes and different vibration periods, together with the recurrence curve for the areal source zone surrounding Banja Luka. The bottom-right plot shows the return periods of the magnitudes that contribute to 50% of the anticipated probabilities of exceedance for the vibration period of 0.1 s and three return periods, *Tr* = 95, 475, and 2475 years, and for the vibration period of 1.0 s and a 475-year return period.

In Figure 8, for the same location, uniform hazard spectra for different combinations of deep geology and local soil conditions are compared to the Eurocode 8 Type 1 spectra (top plots) and Type 2 spectra (bottom plots). Although many civil engineers in Banja Luka would assume that Type 1 spectra should be used (as the 1969 Banja Luka earthquake had a magnitude larger than 5.5), we can see from Figure 8 that the computed UHS amplitudes better fit the Type 2 spectra. The bottom plots also show the ratios between the highest UHS amplitudes and corresponding PGA values. For all the UHS presented, this ratio,

designated as S_{PGA} in Figure 8, differs from the Eurocode 8 factor of 2.5 [19]. In Table 4, we show maximum UHS amplitudes, corresponding vibration periods T, and the S_{PGA} ratios, calculated for different combinations of local soil types and deep geology and for the 10% probability of exceedance in 50 years (the so-called return period Tr = 475 years). Table 4 shows that we did not obtain the Eurocode 8 factor of 2.5 for any combination of local soil types and deep geology conditions. The highest disparity occurs for deep soils on top of geological rock, with S_{PGA} = 4.10, which is 64% greater than Eurocode 8's 2.5 ratio.

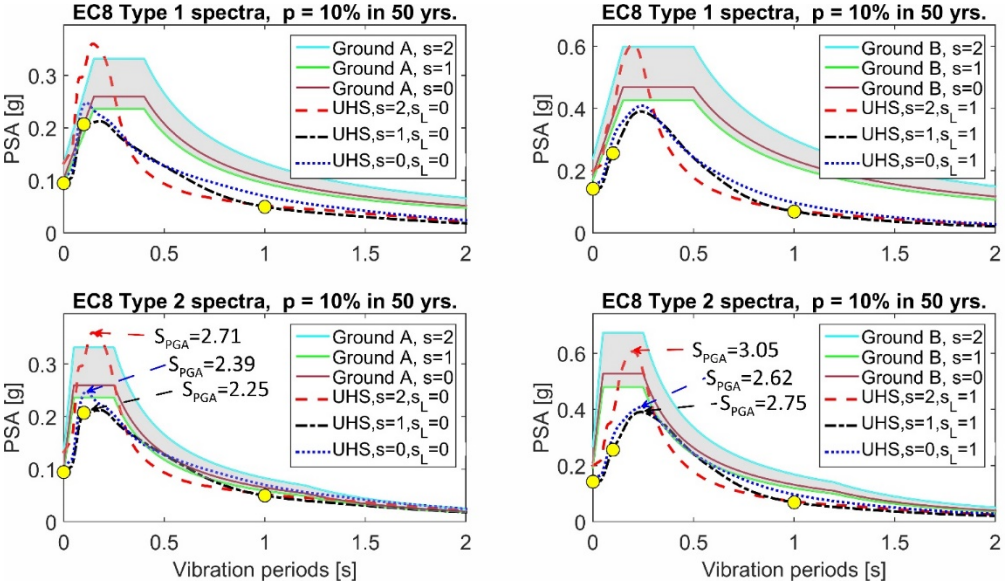

Figure 8. UHS calculated at the 44°46.5′ N, 17°15′ E site, compared to two different Eurocode 8 spectral types [19]. Solid yellow dots show the UHS amplitudes for T = 0.0 (PGA), 0.1, and 1.0 s. Shaded areas contain all possible amplitudes of the Eurocode 8 spectra scaled by the PGA probabilistic estimates for different types of deep geology.

Table 4. Maximum UHS amplitudes for Tr = 475 years, corresponding vibration periods, and the ratios between maximum UHS amplitudes and PGA values (designated as S_{PGA}), calculated for different combinations of site conditions.

	Geological Rock (s = 2)			**Intermediate Sites (s = 1)**			**Deep Geol. Sediments (s = 0)**		
Local Soil	**Max UHS**	***T* for Max UHS**	**S_{PGA}**	**Max UHS**	***T* for Max UHS**	**S_{PGA}**	**Max UHS**	***T* for Max UHS**	**S_{PGA}**
s_L = 0 ("Rock" soil)	0.36 g	0.13 s	2.71	0.21 g	0.09 s	2.25	0.25 g	0.10 s	2.39
s_L = 1 (Stiff soil)	0.61 g	0.20 s	3.05	0.39 g	0.14 s	2.75	0.41 g	0.16 s	2.62
s_L = 2 (Deep soil)	0.44 g	0.11 s	4.10	0.28 g	0.08 s	3.71	0.30 g	0.08 s	3.54

We also tried to simplify the UHS shapes by scaling them with only a couple of amplitudes. Solid yellow dots in Figure 8 show the UHS amplitudes for T = 0.0 (PGA), 0.1, and 1.0 s, which are often proposed for scaling design spectra. However, for the shapes of UHS shown in Figure 8, this is simply not possible. With modern computers, there is no reason why the design spectra should not be calculated directly for all amplitudes for which there are scaling coefficients (in this case, for 61 vibration periods—see Tables A1 and A2).

5. Discussion and Conclusions

In this paper, we estimated and analyzed horizontal UHS for a site in Banja Luka. Banja Luka is situated between the Dinaric Alps and the Pannonian Basin. In addition to geological sediments, Banja Luka has scattered outcrops of deep geological rock and places with complex deep geological strata. Geological sediments close to the investigated location are several hundred meters deep and consist of marls, clays, and sands. There is also a nearby spilite formation and a diabase–chert formation (or metamorphic ophiolitic melange). Banja Luka was also devastated by the 27 October 1969 earthquake.

Regional GMPEs for horizontal *PSA* amplitudes were first described and analyzed. These equations consider both local soil types and deep geological conditions. Using the presented GMPEs, UHS amplitudes were calculated for a site in Banja Luka and compared to the Eurocode 8 [19] spectra.

The primary findings of the study are as follows:

- Effects of the deep geology on the UHS amplitudes are equally important as the local soil effects and should not be neglected.
- The magnitudes that are contributing most to the calculated seismic hazard vary significantly, and depend on the spectral amplitude and the return period, *Tr*.
- The actual return period of the magnitude that contributes most to the calculated seismic hazard is for all vibration periods much shorter than the corresponding return period, *Tr*, which is just a statistical measure (the reciprocal value of the mean annual rate of occurrence); for example, the median contributing magnitude for T = 0.1 s and *Tr* = 475 years had an actual return period of roughly 16 years, while for T = 1.0 s and *Tr* = 475 years it had an actual return period of roughly 143 years.
- In Eurocode 8 terms, it is unclear whether to use Type 1 or Type 2 spectra, as these depend on contributing magnitudes (which can be defined only after a seismic hazard disaggregation, which is rarely or never performed) rather than the absolute maximum event in the vicinity of the studied site.
- The seismic hazard maps that accompany Eurocode 8 should be expressed in terms of probabilities of exceedance only (10% in 10 years or 10% in 50 years), without mentioning the corresponding return periods, *Tr* (95 and 475 years, respectively); in this way we can avoid misunderstanding of the actual most-contributing earthquakes (used to define spectral Type 1 or 2) that have much shorter periods of re-occurrence.
- The ratios between maximum UHS amplitudes and corresponding PGA values differ from the Eurocode 8 factor of 2.5 for all analyzed combinations of deep geology and local soil conditions.
- Design spectra should not be scaled by only one or two amplitudes but rather directly calculated for all amplitudes for which there are scaling coefficients for the GMPE.

We are unable to provide explicit ideas on how to incorporate deep geology into the current codes. Our only suggestion for future Eurocode 8 revisions or proposed guideline adjustments is to allow civil engineers to employ UHS spectra like those shown in Figure 8. In other words, we propose that the Eurocode spectra be generated directly for every specific site using regional GMPEs that account for both deep geology and local soil effects. Modern computers can perform such computations for entire countries, whereas a government-owned server might host UHS spectra for a thick mesh of sites and various combinations of deep geology and local soil conditions.

Although the database utilized to define the GMPEs used for UHS calculations is restricted and the UHS obtained are only preliminary, we suggest that the presented UHS are a step toward more reliable design spectra for Banja Luka and similar regions, and improved reliability of seismic risk estimations for the regional building stock. When new data become available, the GMPEs may be easily updated and the UHS recalculated.

Author Contributions: Conceptualization, B.B., S.L. and S.B.; methodology, B.B. and S.L.; formal analysis, B.B., S.L., S.B. and M.N.; investigation, B.B., S.B., D.R., E.I., M.N. and M.H.-N.; data curation, B.B. and M.H.-N.; writing—original draft preparation, B.B., S.L., S.B. and M.H.-N.; writing—review and editing, B.B., S.L., S.B., D.R., E.I. and M.H.-N.; visualization, B.B. All authors have read and agreed to the published version of the manuscript.

Funding: This research received no external funding.

Institutional Review Board Statement: Not applicable.

Informed Consent Statement: Not applicable.

Data Availability Statement: The original contributions presented in the study are included in the article; further inquiries can be directed to the authors.

Acknowledgments: For the first and third authors, this research has been supported by the Ministry of Science, Technological Development and Innovation (Contract No. 451-03-137/2025-03/200156) and the Faculty of Technical Sciences, University of Novi Sad through the project "Scientific and Artistic Research Work of Researchers in Teaching and Associate Positions at the Faculty of Technical Sciences, University of Novi Sad 2025" (No. 01-50/295).

Conflicts of Interest: The authors declare no conflicts of interest.

Abbreviations

The following abbreviations are used in this manuscript:

a_g	Horizontal PGA value from the official seismic hazard map
EC8	Eurocode 8
GMPE	Ground motion prediction equations
$N(a)$	Mean yearly rate of occurrence of seismic events that cause a ground motion *PSA* amplitude to exceed an expectation "*a*"
$p(a)$	Probability that a ground motion *PSA* amplitude will surpass the expectation *a* at least once in *t* years
$P(a)$	Probability of at least one yearly surpassing of the expectation a
PGA	Peak ground acceleration
PSA	Pseudo-absolute acceleration spectra
PSHA	Probabilistic seismic hazard assessment
s	Deep geology parameter
S	Soil factor according to Eurocode 8
s_L	Local soil parameter
S_{PGA}	Ratio of the maximum UHS amplitude to PGA
Tr	Return period
UHS	Uniform hazard spectra
USC	University of Southern California
USC-CA	GMPEs for California, derived by researchers from USC
USC-ExYU	GMPEs for ex-Yugoslavia, derived by researchers from USC
$V_{S,30}$	Average shear wave velocity in the top 30 m of the local soil

Appendix A. Scaling Coefficients for Horizontal *PSA*

Table A1. Scaling coefficients of the GMPEs for horizontal *PSA*, computed using the strong motion data recorded at all distances in the northwestern Balkans—Equation (1).

T	c_1	c_2	c_3	R_0	c_4	c_5	c_6	c_7	σ_{log}
0.040	−1.098	0.363	−1.349	19.8	0.142	−0.067	−0.173	−0.123	0.266
0.042	−1.073	0.362	−1.352	19.9	0.139	−0.065	−0.175	−0.124	0.267
0.044	−1.048	0.360	−1.356	20.0	0.135	−0.063	−0.178	−0.126	0.268
0.046	−1.018	0.358	−1.360	20.1	0.132	−0.062	−0.181	−0.128	0.269
0.048	−0.971	0.355	−1.365	20.2	0.126	−0.060	−0.190	−0.136	0.270
0.050	−0.921	0.352	−1.371	20.3	0.120	−0.058	−0.198	−0.143	0.272
0.055	−0.810	0.345	−1.387	20.6	0.107	−0.053	−0.214	−0.156	0.275
0.060	−0.713	0.340	−1.404	21.0	0.096	−0.048	−0.224	−0.164	0.278
0.065	−0.627	0.337	−1.424	21.3	0.085	−0.043	−0.228	−0.167	0.282
0.070	−0.552	0.335	−1.446	21.7	0.076	−0.037	−0.227	−0.164	0.285
0.075	−0.511	0.337	−1.466	22.1	0.071	−0.032	−0.212	−0.147	0.286
0.080	−0.491	0.340	−1.487	22.5	0.071	−0.026	−0.194	−0.128	0.287
0.085	−0.484	0.346	−1.507	22.8	0.074	−0.021	−0.178	−0.110	0.287
0.090	−0.479	0.351	−1.525	23.0	0.079	−0.015	−0.168	−0.099	0.286
0.095	−0.472	0.356	−1.541	23.3	0.085	−0.009	−0.165	−0.094	0.287
0.100	−0.467	0.360	−1.552	23.5	0.092	−0.003	−0.168	−0.096	0.287
0.110	−0.457	0.368	−1.566	23.7	0.110	0.008	−0.187	−0.113	0.288
0.120	−0.434	0.374	−1.582	24.1	0.130	0.020	−0.210	−0.139	0.287
0.130	−0.407	0.380	−1.599	24.7	0.151	0.032	−0.230	−0.165	0.286
0.140	−0.395	0.387	−1.621	25.3	0.170	0.044	−0.234	−0.180	0.284
0.150	−0.406	0.396	−1.638	25.8	0.188	0.056	−0.232	−0.188	0.283
0.160	−0.444	0.405	−1.644	26.0	0.205	0.068	−0.227	−0.192	0.284
0.170	−0.495	0.413	−1.645	25.9	0.221	0.079	−0.221	−0.193	0.285
0.180	−0.555	0.421	−1.640	25.6	0.234	0.091	−0.215	−0.193	0.287
0.190	−0.624	0.427	−1.628	25.1	0.246	0.102	−0.209	−0.190	0.288
0.200	−0.699	0.433	−1.611	24.5	0.256	0.113	−0.203	−0.186	0.290
0.220	−0.864	0.441	−1.567	23.1	0.277	0.134	−0.187	−0.169	0.291
0.240	−1.044	0.449	−1.521	21.8	0.296	0.153	−0.156	−0.136	0.292
0.260	−1.233	0.457	−1.477	20.6	0.311	0.172	−0.115	−0.094	0.292
0.280	−1.435	0.468	−1.434	19.6	0.322	0.188	−0.069	−0.051	0.294
0.300	−1.643	0.480	−1.391	18.6	0.327	0.203	−0.025	−0.013	0.297
0.320	−1.853	0.492	−1.347	17.6	0.330	0.216	0.016	0.020	0.301
0.340	−2.049	0.505	−1.306	16.5	0.330	0.227	0.047	0.043	0.305
0.360	−2.224	0.517	−1.271	15.4	0.328	0.236	0.070	0.060	0.309
0.380	−2.375	0.529	−1.244	14.5	0.324	0.243	0.087	0.075	0.311
0.400	−2.499	0.540	−1.226	13.8	0.318	0.248	0.100	0.087	0.313
0.420	−2.603	0.550	−1.215	13.2	0.310	0.250	0.109	0.098	0.314
0.440	−2.686	0.559	−1.211	12.9	0.302	0.250	0.118	0.109	0.314
0.460	−2.760	0.566	−1.207	12.6	0.295	0.248	0.124	0.119	0.314
0.480	−2.828	0.573	−1.203	12.4	0.287	0.244	0.130	0.128	0.314
0.500	−2.883	0.579	−1.201	12.3	0.279	0.238	0.134	0.136	0.315
0.550	−3.009	0.588	−1.185	12.1	0.262	0.216	0.138	0.153	0.316
0.600	−3.118	0.592	−1.157	12.0	0.248	0.186	0.134	0.163	0.319
0.650	−3.225	0.594	−1.118	11.7	0.233	0.147	0.118	0.167	0.322
0.700	−3.321	0.594	−1.078	11.3	0.216	0.103	0.092	0.165	0.323
0.750	−3.410	0.596	−1.044	10.9	0.198	0.057	0.066	0.162	0.323
0.800	−3.497	0.598	−1.012	10.4	0.183	0.011	0.043	0.157	0.323
0.850	−3.581	0.600	−0.984	9.9	0.170	−0.028	0.023	0.152	0.323

Table A1. *Cont.*

T	c_1	c_2	c_3	R_0	c_4	c_5	c_6	c_7	σ_{log}
0.900	−3.658	0.602	−0.959	9.5	0.159	−0.059	0.006	0.145	0.322
0.950	−3.728	0.604	−0.936	9.2	0.150	−0.082	−0.008	0.137	0.322
1.000	−3.792	0.604	−0.911	8.9	0.141	−0.098	−0.021	0.129	0.322
1.100	−3.899	0.603	−0.864	8.6	0.128	−0.117	−0.040	0.109	0.323
1.200	−3.976	0.600	−0.825	8.5	0.115	−0.132	−0.056	0.089	0.323
1.300	−4.028	0.596	−0.796	8.6	0.102	−0.160	−0.069	0.072	0.324
1.400	−4.069	0.592	−0.778	8.7	0.089	−0.196	−0.079	0.061	0.323
1.500	−4.110	0.590	−0.768	8.6	0.077	−0.227	−0.085	0.054	0.323
1.600	−4.152	0.590	−0.766	8.6	0.069	−0.238	−0.089	0.048	0.323
1.700	−4.192	0.590	−0.770	8.7	0.064	−0.220	−0.090	0.046	0.322
1.800	−4.228	0.592	−0.782	8.8	0.061	−0.191	−0.089	0.046	0.322
1.900	−4.263	0.595	−0.800	8.8	0.061	−0.173	−0.084	0.048	0.322
2.000	−4.295	0.599	−0.825	9.0	0.063	−0.184	−0.077	0.052	0.322

Table A2. Scaling coefficients of the GMPEs for horizontal *PSA*, computed using the strong motion data in the northwestern Balkans, recorded at distances up to 30 km—Equation (1).

T	c_1	c_2	c_3	R_0	c_4	c_5	c_6	c_7	σ_{log}
0.040	3.047	0.362	−3.639	40.0	0.090	−0.067	−0.258	−0.116	0.266
0.042	3.044	0.360	−3.626	40.0	0.087	−0.065	−0.261	−0.117	0.266
0.044	3.041	0.358	−3.612	40.0	0.083	−0.063	−0.263	−0.118	0.267
0.046	3.041	0.356	−3.598	40.0	0.079	−0.062	−0.267	−0.121	0.268
0.048	3.056	0.353	−3.583	40.0	0.073	−0.060	−0.278	−0.130	0.270
0.050	3.067	0.350	−3.565	40.0	0.066	−0.058	−0.288	−0.138	0.272
0.055	3.088	0.343	−3.526	40.0	0.052	−0.053	−0.308	−0.153	0.276
0.060	3.093	0.338	−3.488	40.0	0.039	−0.048	−0.320	−0.160	0.280
0.065	3.088	0.335	−3.454	40.0	0.029	−0.043	−0.324	−0.160	0.284
0.070	3.065	0.333	−3.421	40.0	0.021	−0.037	−0.319	−0.152	0.288
0.075	2.987	0.334	−3.374	40.0	0.017	−0.032	−0.297	−0.125	0.289
0.080	2.940	0.337	−3.358	40.0	0.015	−0.026	−0.272	−0.094	0.289
0.085	2.907	0.341	−3.355	40.0	0.015	−0.021	−0.249	−0.064	0.289
0.090	2.881	0.346	−3.355	40.0	0.015	−0.015	−0.234	−0.042	0.289
0.095	2.857	0.350	−3.352	40.0	0.017	−0.009	−0.227	−0.030	0.288
0.100	2.826	0.354	−3.340	40.0	0.020	−0.003	−0.230	−0.026	0.288
0.110	2.701	0.362	−3.271	40.0	0.029	0.008	−0.252	−0.041	0.287
0.120	2.480	0.370	−3.138	40.0	0.046	0.020	−0.285	−0.074	0.285
0.130	2.258	0.378	−3.010	40.0	0.068	0.032	−0.312	−0.111	0.283
0.140	2.101	0.386	−2.936	40.0	0.090	0.044	−0.320	−0.133	0.279
0.150	2.000	0.396	−2.902	40.0	0.110	0.056	−0.321	−0.147	0.277
0.160	1.981	0.404	−2.918	40.0	0.128	0.068	−0.317	−0.155	0.278
0.170	1.999	0.411	−2.957	40.0	0.145	0.079	−0.310	−0.160	0.280
0.180	2.030	0.416	−2.999	40.0	0.160	0.091	−0.303	−0.162	0.281
0.190	2.049	0.421	−3.031	40.0	0.173	0.102	−0.297	−0.162	0.283
0.200	2.045	0.424	−3.046	40.0	0.185	0.113	−0.290	−0.161	0.284
0.220	1.988	0.430	−3.047	40.0	0.210	0.134	−0.270	−0.146	0.285
0.240	1.957	0.436	−3.083	40.0	0.240	0.153	−0.233	−0.113	0.284
0.260	2.023	0.446	−3.196	40.0	0.268	0.172	−0.183	−0.071	0.283
0.280	2.267	0.460	−3.435	40.0	0.288	0.188	−0.128	−0.027	0.285
0.300	2.654	0.475	−3.764	40.0	0.298	0.203	−0.078	0.013	0.288
0.320	3.151	0.492	−4.162	40.0	0.302	0.216	−0.031	0.048	0.292
0.340	3.682	0.509	−4.568	40.0	0.300	0.227	0.001	0.071	0.296
0.360	4.191	0.524	−4.952	40.0	0.295	0.236	0.023	0.087	0.300

Table A2. *Cont.*

T	c_1	c_2	c_3	R_0	c_4	c_5	c_6	c_7	σ_{log}
0.380	4.644	0.538	−5.293	40.0	0.287	0.243	0.039	0.099	0.302
0.400	5.024	0.551	−5.583	40.0	0.278	0.248	0.051	0.108	0.304
0.420	5.345	0.564	−5.831	40.0	0.270	0.250	0.059	0.114	0.305
0.440	5.581	0.575	−6.026	40.0	0.265	0.250	0.069	0.121	0.306
0.460	5.783	0.585	−6.195	40.0	0.261	0.248	0.078	0.127	0.307
0.480	5.934	0.593	−6.331	40.0	0.260	0.244	0.088	0.133	0.308
0.500	6.038	0.601	−6.434	40.0	0.259	0.238	0.095	0.138	0.309
0.550	6.150	0.615	−6.591	40.0	0.264	0.216	0.112	0.149	0.312
0.600	6.145	0.624	−6.656	40.0	0.272	0.186	0.118	0.155	0.313
0.650	6.143	0.627	−6.699	40.0	0.268	0.147	0.106	0.156	0.313
0.700	6.138	0.628	−6.721	40.0	0.254	0.103	0.082	0.154	0.312
0.750	6.169	0.628	−6.757	40.0	0.234	0.057	0.056	0.150	0.311
0.800	6.202	0.629	−6.795	40.0	0.214	0.011	0.030	0.146	0.310
0.850	6.218	0.630	−6.825	40.0	0.197	−0.028	0.007	0.141	0.310
0.900	6.193	0.633	−6.831	40.0	0.183	−0.059	−0.013	0.134	0.310
0.950	6.121	0.634	−6.807	40.0	0.172	−0.082	−0.031	0.126	0.309
1.000	6.004	0.635	−6.753	40.0	0.164	−0.098	−0.047	0.115	0.309
1.100	5.668	0.636	−6.576	40.0	0.151	−0.117	−0.074	0.092	0.307
1.200	5.264	0.635	−6.351	40.0	0.141	−0.132	−0.098	0.066	0.305
1.300	4.876	0.634	−6.130	40.0	0.131	−0.160	−0.119	0.041	0.302
1.400	4.612	0.632	−5.984	40.0	0.121	−0.196	−0.135	0.021	0.301
1.500	4.433	0.632	−5.895	40.0	0.112	−0.227	−0.146	0.007	0.302
1.600	4.279	0.633	−5.825	40.0	0.106	−0.238	−0.154	−0.004	0.302
1.700	4.158	0.635	−5.779	40.0	0.101	−0.220	−0.159	−0.012	0.304
1.800	4.072	0.637	−5.758	40.0	0.098	−0.191	−0.160	−0.017	0.305
1.900	4.020	0.640	−5.759	40.0	0.097	−0.173	−0.159	−0.019	0.308
2.000	3.998	0.644	−5.783	40.0	0.098	−0.184	−0.154	−0.017	0.311

References

1. Trifunac, M.D.; Brady, A.G. On the correlation of seismic intensity scales with the peaks of recorded strong ground motion. *Bull. Seismol. Soc. Am.* **1975**, *65*, 139–162.
2. Ermert, L.; Poggi, V.; Burjánek, J.; Fäh, D. Fundamental and higher two-dimensional resonance modes of an Alpine valley. *Geophys. J. Int.* **2014**, *198*, 795–811. [CrossRef]
3. Faccioli, E.; Vanini, M. Complex seismic site effects in sediment-filled valleys and implications on design spectra. *Prog. Struct. Eng. Mater.* **2003**, *5*, 223–238. [CrossRef]
4. Stamati, O.; Klimis, N.; Lazaridis, T. Evidence of complex site effects and soil non-linearity numerically estimated by 2D vs 1D seismic response analyses in the city of Xanthi. *Soil Dyn. Earthq. Eng.* **2016**, *87*, 101–115. [CrossRef]
5. Zhu, C.; Chávez-García, F.J.; Thambiratnam, D.; Gallage, C. Quantifying the edge-induced seismic aggravation in shallow basins relative to the 1D SH modelling. *Soil Dyn. Earthq. Eng.* **2018**, *115*, 402–412. [CrossRef]
6. Zhu, C.; Thambiratnam, D. Interaction of geometry and mechanical property of trapezoidal sedimentary basins with incident SH waves. *Bull. Earthq. Eng.* **2016**, *14*, 2977–3002. [CrossRef]
7. Zhu, C.; Thambiratnam, D.P.; Zhang, J. Response of sedimentary basin to obliquely incident SH waves. *Bull. Earthq. Eng.* **2016**, *14*, 647–671. [CrossRef]
8. Bulajić, B.Đ.; Hadzima-Nyarko, M.; Pavić, G. Vertical to Horizontal UHS Ratios for Low to Medium Seismicity Regions with Deep Soil atop Deep Geological Sediments—An Example of the City of Osijek, Croatia. *Appl. Sci.* **2021**, *11*, 6782. [CrossRef]
9. Bulajić, B.Đ.; Hadzima-Nyarko, M.; Pavić, G. Horizontal UHS Amplitudes for Regions with Deep Soil Atop Deep Geological Sediments—An Example of Osijek, Croatia. *Appl. Sci.* **2021**, *11*, 6296. [CrossRef]
10. Bulajic, B.Đ.; Hadzima-Nyarko, M.; Pavic, G. PGA estimates for deep soils atop deep geological sediments -An example of Osijek, Croatia. *Geomech. Eng.* **2022**, *30*, 233–246. [CrossRef]
11. Bulajić, B.Đ.; Pavić, G.; Hadzima-Nyarko, M. PGA vertical estimates for deep soils and deep geological sediments—A case study of Osijek (Croatia). *Comput. Geosci.* **2022**, *158*, 104985. [CrossRef]
12. Bulajić, B.Đ.; Bajić, S.; Stojnić, N. The effects of geological surroundings on earthquake-induced snow avalanche prone areas in the Kopaonik region. *Cold Reg. Sci. Technol.* **2018**, *149*, 29–45. [CrossRef]

13. Douglas, J. Earthquake ground motion estimation using strong-motion records: A review of equations for the estimation of peak ground acceleration and response spectral ordinates. *Earth-Sci. Rev.* **2003**, *61*, 43–104. [CrossRef]
14. Peng, Y.; Wang, Z.; Woolery, E.W.; Lyu, Y.; Carpenter, N.S.; Fang, Y.; Huang, S. Ground-motion site effect in the Beijing metropolitan area. *Eng. Geol.* **2020**, *266*, 105395. [CrossRef]
15. Lee, V.W.; Manić, M.I.; Bulajić, B.Đ.; Herak, D.; Herak, M.; Trifunac, M.D. Microzonation of Banja Luka for performance-based earthquake-resistant design. *Soil Dyn. Earthq. Eng.* **2015**, *78*, 71–88. [CrossRef]
16. Lee, V.W.; Trifunac, M.D.; Bulajić, B.Đ. Seismic microzoning in Novi Sad, Serbia—A case study in a low-seismicity region that is exposed to large and distant earthquakes. *J. Seismol.* **2023**, *27*, 979–997. [CrossRef]
17. Lee, V.W.; Trifunac, M.D.; Bulajić, B.Đ. Seismic hazard mapping for peak ground velocity: Microzonation of Novi Sad, Serbia—A case study in a low-seismicity region exposed to large and distant earthquakes. *J. Seismol.* **2025**, *29*, 85–105. [CrossRef]
18. Lee, V.W.; Trifunac, M.D.; Bulajić, B.Đ.; Manić, M.I.; Herak, D.; Herak, M.; Dimov, G.; Gičev, V. Seismic microzoning of Štip in Macedonia. *Soil Dyn. Earthq. Eng.* **2017**, *98*, 54–66. [CrossRef]
19. *European Standard EN 1998-1:2004*; Eurocode 8: Design of Structures for Earthquake Resistance. Part 1: General Rules, Seismic Actions and Rules for Buildings. CEN: Brussels, Belgium, 2004.
20. Seismic Zone Maps and Reference Ground Accelerations Therein of B&H. Maps Accompanying National Annexes (NA). B&H. 2018. Available online: http://eurokodovi.ba/seizmika/ (accessed on 1 May 2025).
21. Ademović, N.; Demir, V.; Cvijić-Amulić, S.; Málek, J.; Prachař, I.; Vackář, J. Compilation of the seismic hazard maps in Bosnia and Herzegovina. *Soil Dyn. Earthq. Eng.* **2021**, *141*, 106500. [CrossRef]
22. Ademović, N.; Demir, V.; Cvijić-Amulić, S.; Málek, J.; Prachař, I.; Vackář, J. Corrigendum to "Compilation of the seismic hazard maps in Bosnia and Herzegovina" [Soil Dynam. Earthq. Eng. 141 (2021) 106500]. *Soil Dyn. Earthq. Eng.* **2023**, *164*, 107633. [CrossRef]
23. Ustaszewski, K.; Herak, M.; Tomljenović, B.; Herak, D.; Matej, S. Neotectonics of the Dinarides–Pannonian Basin transition and possible earthquake sources in the Banja Luka epicentral area. *J. Geodyn.* **2014**, *82*, 52–68. [CrossRef]
24. Hrvatović, H. *Geological Guidebook through Bosnia and Herzegovina*; Geological Survey of Bosnia and Herzegovina: Sarajevo, Bosnia and Herzegovina, 2006; p. 163.
25. USGS. *Earthquake Catalogue for all Earthquakes with Mw ≥ 3.0 in the Period Between 1900 and April 2025 for the Geographic Region between 41° N and 47° N, and 13° E and 23° E*; USGS: Reston, VA, USA, 2025.
26. Mojičević, M.; Vilovski, S.; Tomić, B. *Basic Geological Map—Banja Luka, L 33-119 (in Serbian: Osnovna Geološka Karta SFRJ, BANJA LUKA, L 33-119)*; Federal Geological Survey: Belgrade, Serbia, 1976.
27. Seed, H.B.; Murarka, R.; Lysmer, J.; Idriss, I.M. Relationships of maximum acceleration, maximum velocity, distance from source, and local site conditions for moderately strong earthquakes. *Bull. Seismol. Soc. Am.* **1976**, *66*, 1323–1342.
28. Seed, H.B.; Ugas, C.; Lysmer, J. Site-dependent spectra for earthquake-resistant design. *Bull. Seismol. Soc. Am.* **1976**, *66*, 221–243. [CrossRef]
29. Lee, V.W.; Trifunac, M.D.; Bulajić, B.D.; Manić, M.I.; Herak, D.; Herak, M.; Dimov, G. Seismic microzoning in Skopje, Macedonia. *Soil Dyn. Earthq. Eng.* **2017**, *98*, 166–182. [CrossRef]
30. Jordanovski, L.R.; Lee, V.W.; Manić, M.I.; Olumčeva, T.; Sinadnovski, C.; Todorovska, M.I.; Trifunac, M.D. *Strong Earthquake Ground Motion Data in EQINFOS: Yugoslavia. Part I*; Department of Civil Engineering, University of Southern California: Los Angeles, CA, USA, 1987.
31. Ambraseys, N.; Douglas, J.; Margaris, B.; Sigbjörnsson, R.; Berge-Thierry, C.; Suhadolc, P.; Costa, G.; Smit, P. Dissemination of European strong-motion data. In Proceedings of the 13th World Conference on Earthquake Engineering, Vancouver, BC, Canada, 1–6 August 2004.
32. Ambraseys, N.; Douglas, J.; Margaris, B.; Sigbjörnsson, R.; Smit, P.; Suhadolc, P. Internet site for European strong motion data. In Proceedings of the 12th European Conference on Earthquake Engineering, London, UK, 9–13 September 2002.
33. Bulajić, B.Đ.; Manić, M.I.; Lađinović, Đ. Effects of shallow and deep geology on seismic hazard estimates: A case study of pseudo-acceleration response spectra for the northwestern Balkans. *Nat. Hazards* **2013**, *69*, 573–588. [CrossRef]
34. Giardini, D.; Woessner, J.; Danciu, L.; Crowley, H.; Cotton, F.; Grünthal, G.; Pinho, R.; Valensise, L.; Consortium, S. *European Seismic Hazard Map for Peak Ground Acceleration, 10% Exceedance Probabilities in 50 Years*; Swiss Seismological Service: Zurich, Switzerland, 2013.
35. Woessner, J.; Laurentiu, D.; Giardini, D.; Crowley, H.; Cotton, F.; Grünthal, G.; Valensise, G.; Arvidsson, R.; Basili, R.; Demircioglu, M.B.; et al. The 2013 European Seismic Hazard Model: Key components and results. *Bull. Earthq. Eng.* **2015**, *13*, 3553–3596. [CrossRef]
36. Pagani, M.; Garcia-Pelaez, J.; Gee, R.; Johnson, K.; Poggi, V.; Styron, R.; Weatherill, G.; Simionato, M.; Viganò, D.; Danciu, L.; et al. *Global Earthquake Model (GEM) Seismic Hazard Map (version 2018.1–December 2018)*; GEM Foundation: Pavia, Italy, 2018.

37. Stucchi, M.; Rovida, A.; Gomez Capera, A.A.; Alexandre, P.; Camelbeeck, T.; Demircioglu, M.B.; Gasperini, P.; Kouskouna, V.; Musson, R.M.W.; Radulian, M.; et al. The SHARE European Earthquake Catalogue (SHEEC) 1000–1899. *J. Seismol.* **2013**, *17*, 523–544. [CrossRef]
38. Grünthal, G.; Wahlström, R. The European-Mediterranean Earthquake Catalogue (EMEC) for the last millennium. *J. Seismol.* **2012**, *16*, 535–570. [CrossRef]
39. Grünthal, G.; Wahlström, R.; Stromeyer, D. The SHARE European Earthquake Catalogue (SHEEC) for the time period 1900–2006 and its comparison to the European-Mediterranean Earthquake Catalogue (EMEC). *J. Seismol.* **2013**, *17*, 1339–1344. [CrossRef]
40. Chioccarelli, E.; Cito, P.; Iervolino, I.; Giorgio, M. REASSESS V2.0: Software for single- and multi-site probabilistic seismic hazard analysis. *Bull. Earthq. Eng.* **2019**, *17*, 1769–1793. [CrossRef]
41. Cornell, C.A. Engineering seismic risk analysis. *Bull. Seismol. Soc. Am.* **1968**, *58*, 1583–1606. [CrossRef]
42. McGuire, R.K. *FORTRAN Computer Program for Seismic Risk Analysis*; Open-File Report 76–67; U.S. Geological Survey: Reston, VA, USA, 1976.
43. Ang, A.H.; Tang, W.H. *Probability Concepts in Engineering Planning: Emphasis on Applications to Civil and Environmental Engineering*; John Wiley and Sons: Hoboken, NJ, USA, 2007.
44. Bazzurro, P.; Allin Cornell, C. Disaggregation of seismic hazard. *Bull. Seismol. Soc. Am.* **1999**, *89*, 501–520. [CrossRef]
45. McGuire, R.K. Probabilistic seismic hazard analysis and design earthquakes: Closing the loop. *Bull. Seismol. Soc. Am.* **1995**, *85*, 1275–1284. [CrossRef]